Sensors and Materials, Vol. 11, No. 1 (1999) 021–029
MYU Tokyo

S & M 0352

$Cu(In,Ga)Se_2$ Thin-Film Photosensors

Tokio Nakada, Masakazu Fukuda, Morihide Yamanaka[1] and Akio Kunioka

Department of Electrical Engineering and Electronics, Aoyama Gakuin University,
Setagaya-ku, Tokyo 157, Japan
[1]Moririca Electric Limited, Izumi, Yokohama 245 Japan

(Received December 30, 1997; accepted October 2, 1998)

Key words: $Cu(In,Ga)Se_2$, photosensors, thin film, photovoltaic detectors, wide spectral response, radiation-hardened sensors

Photovoltaic sensors with a $Cu(In,Ga)Se_2$ (CIGS) thin film, a promising material for use in radiation-hardened space devices, have been investigated for the first time. Linear light-current characteristics were observed for the CIGS photosensors under illumination intensities ranging from 1 to 10^3 lux. The photoresponse time was measured to be approximately 3 μs, which is comparable to that of crystalline silicon pn junction and amorphous silicon pin junction photosensors. However, the reverse saturation current was relatively large, 10^{-7} A/cm^2, in the present experiment. The spectral response was observed in the wavelength range of 400–1,200 nm, suggesting that this device may be utilized as a photosensor with a wide spectral response.

1. Introduction

Polycrystalline $Cu(In_{x-1}Ga_x)Se_2$ (CIGS) thin films have several advantages including the following. (1) A large optical absorption coefficient (~10^5 cm^{-1}) which allows fabrication of thin film electrooptical devices since sufficient light is absorbed even in thin film form. (2) The optical band gap of CIGS absorber layers can be controlled from 1.04 to 1.68 eV by changing the gallium content x = Ga / (In+Ga). This means that the cutoff wavelength in the spectral response curve of photovoltaic devices varies from 0.74 to 1.19 μm if the Ga content is uniform through inside of CIGS layers. (3) P-type electrical conduction can be realized by controlling the copper (Cu)/indium (In) atomic ratio. These properties enable fabrication of a photosensor with a wide spectral response. In fact, $CuInSe_2$ (CIS) /CdS heterojunction photovoltaic detectors with evaporated cadmium

sulfide (CdS) thin film on single crystal CIS has been fabricated by the Bell Telephone Laboratories group.[1] In their results, the Bell group reported that fabricated devices displayed uniform quantum efficiencies of up to ~70% between 550 and 1250 nm. However, no detailed data regarding photoresponse time, dark reverse saturation current and illumination intensity dependence of photocurrent have been demonstrated. Furthermore, no photosensor fabricated using polycrystalline CIGS thin films has been reported to date, although there have been several reports on high-efficiency solar cells using this material.[2,3] On the other hand, NASDA (National Space Development Agency of Japan) group[4] have recently revealed that CIGS solar cells exhibited a superior hardness against electron or proton radiations. This result suggests that the CIGS photosensor also has a potential for use in radiation-hardened space devices.

We thus have investigated device structures and the photoelectric characteristics of CIGS thin film photosensors. In this paper, device structure and preliminary performance characteristics such as spectral response, photoresponse time, and reverse saturation current are presented.

2. Structure and Fabrication of CIGS Photosensors

The structure of a CIGS photosensor is shown in Fig. 1, which consists of a CIGS absorber layer with p-type conduction, a CdS buffer layer, semi-insulating zinc oxide (i-ZnO), and a transparent conducting aluminum-doped zinc oxide (ZnO:Al) layer. The selenized CIGS (2 μm)/Mo (0.8 μm)/glass substrates were supplied by Showa Shell Sekiyu

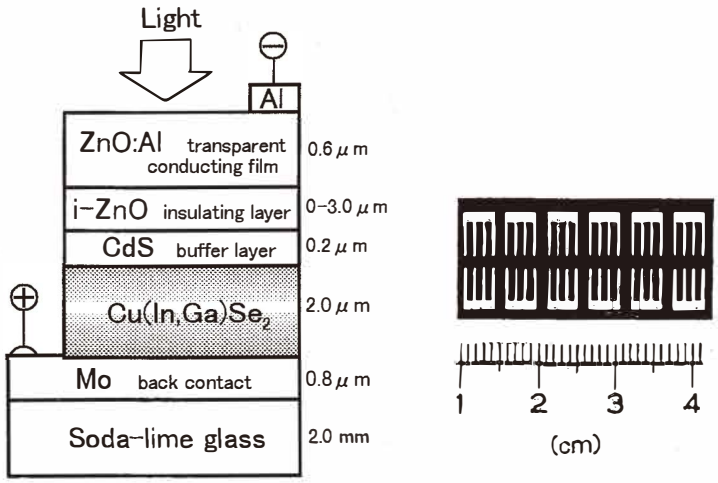

Fig. 1. The structure of a CIGS thin film photosensor. Twelve photosensors with an active area of 0.2 cm^2 are fabricated on the glass substrate.

K. K. Central Laboratory. As described in a previous paper,[5] standard CIGS material is fabricated by selenization of sputter-deposited In/(Cu-Ga) alloy precursor layers and surface sulfurization of a CIGS layer. The absorber layer with a graded Ga content has sulfur near the front face. Typical film thickness was around 2.0 μm. A 0.2-μm-thick CdS buffer layer was then grown onto the CIGS/Mo/glass substrates by the chemical bath deposition (CBD) technique.[6] The CdS film exhibited a resistivity of 1.3×10^8 Ω·cm and an optical transmission of approximately 80% in the wavelength range from 600 to 1,300 nm. An i-ZnO layer was then deposited onto the CdS layers by rf magnetron sputtering using substrate temperatures in the range of 25–80°C in a mixture of O_2-Ar. As-fabricated films showed resistivities of 2.5×10^8 Ω·cm and optical transmission of more than 80% in wavelengths ranging from 500 to 1300 nm. A 0.6-μm-thick ZnO:Al layer was also deposited onto the i-ZnO layer by rf magnetron sputtering in Ar gas using substrate temperatures in the range of 25–70°C. As-fabricated films exhibited low resistivity of 6×10^{-4} Ω·cm and a relatively high optical transmission of more than 80% in the wavelengths ranging from 400 to 900 nm. Finally, the CIGS sensor was completed by vacuum deposition of an Al front electrode.

As can be seen in Fig. 1, the structure of a CIGS photosensor is exactly the same as CIGS solar cells, except for the thickness of the CdS buffer and i-ZnO layers. For device engineering purposes the junction model of these devices is complicated and is under investigation at present. Schmid *et al.*[7] have proposed a buried junction model of CIS solar cells with p-type $CuInSe_2$ and n-type $CuIn_3Se_5$ which exists at the surface region of the CIS absorber layer. However, the carrier concentration of $CuIn_3Se_5$ is too low to fabricate high-efficiency solar cells. Recently, the NREL (National Renewable Energy Laboratory, USA) group[8] has demonstrated that the interfacial reaction that occurs during the chemical bath deposition of the CdS buffer layer is instrumental in creating a buried n-CIS:Cd/p-CIS homo-junction in CIS-based absorbers. The CdS buffer layer provides a good lattice match to the CIS, a possible compositional grading at the interface region, shielding from the damage during sputtering of ZnO as well as the Cd doping. On the other hand, the role of semi-insulating ZnO is an improvement of open circuit voltage for solar cells due to a decrease in the leakage current of the diode by an increase in shunt resistance.

3. Characteristics of CIGS Photosensors

3.1 *Spectral response*

Figure 2 shows the spectral response curve of a thin film CIGS sensor with 0.1-μm-thick i-ZnO layer. The sensor showed good spectral response between 400 and 1,300 nm, suggesting the possibility of a photosensor with a wide spectral response. Little dependence on i-ZnO layer thickness was observed in the spectral response curves, since the optical absorption of i-ZnO is very low in this wavelength region. The short wavelength cutoff is attributed to the absorption of CdS layer whose band-gap energy is 2.4 eV. The photocurrent may be improved by replacing the CdS layer with other wider band-gap materials such as zinc sulfide (ZnS). The long wavelength falloff is due to the fundamental absorption limit of CIGS. The decrease in quantum efficiency at wavelengths above

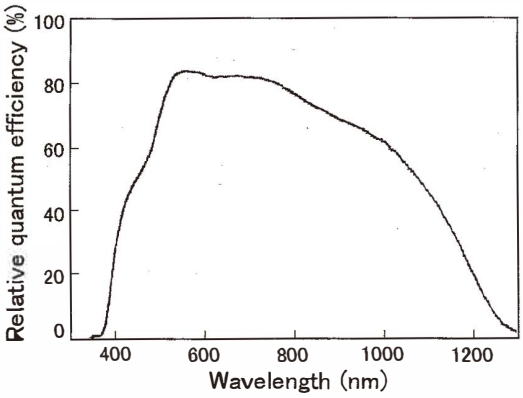

Fig. 2. The spectral response curve of a CIGS thin film photosensor with 1.0-μm-thick i-ZnO layers.

800 nm is attributed to free carrier absorption in the ZnO:Al layer. The photocurrent in the long wavelength region may be improved by replacing the ZnO:Al layer with a ZnO:B layer, since ZnO:B possesses a higher electron mobility.[9]

3.2 *Dark reverse saturation current density* (J_0)

Figure 3 shows the current density versus voltage (*J-V*) characteristics measured at room temperature for CIGS sensors with i-ZnO layers of varying thickness. The dark reverse saturation current density J_0 decreased as i-ZnO layer thickness increased and showed a minimum J_0 of 3.2×10^{-7} A/cm^2 at a 3.0-μm-thick i-ZnO layer. The decrease in J_0 is mainly attributed to the increase in shunt resistance of the diode due to the increase in resistance of i-ZnO layer, which results in the decrease in leakage current. The J_0, therefore, can be improved by increasing the thickness of i-ZnO layer. The J_0 also decreased as the oxygen concentration in an Ar-O_2 mixture increased during sputtering since the resistivity of ZnO layer increased by increased oxygen concentration due to the compensation of oxygen vacancies which act as donors in the ZnO matrix. On the other hand, the forward current density (*J*) showed a straight line at bias voltages of 0.2–0.4 V, since, if the forward voltage is higher than kT/q, *J* increased exponentially by increasing the forward voltage.[10] The decrease in current density at voltage ranges above 0.5 V is attributable to the increase in the series resistance of the diode. Figure 4 shows the dark *J-V* characteristics measured at different temperatures for CIGS photosensors with i-ZnO layer thickness of 3.0 μm. As can be seen, J_0 increased as the ambient temperature increased. This is more clearly observed in Fig. 5, showing that the ln J_0 decreased with increasing the reverse of ambient temperature *T*. This behavior can be explained by the following equation.[10]

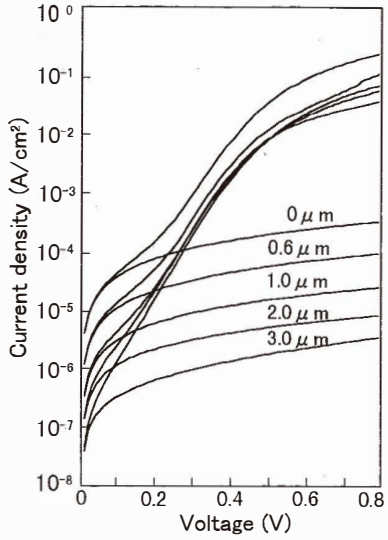

Fig. 3. The *J-V* characteristics measured at room temperature for CIGS thin film photosensors with i-ZnO layers of varying thickness ranging from 0 to 3.0 μm.

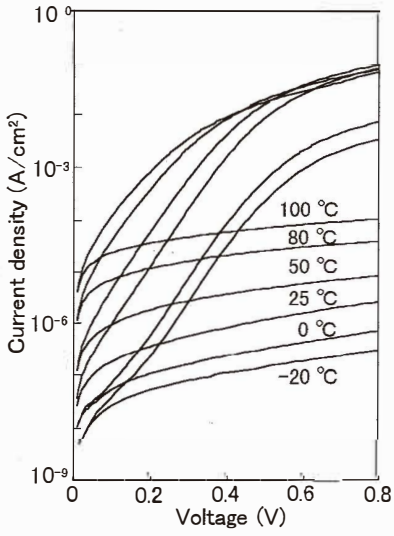

Fig. 4. The dark *J-V* characteristics measured at different temperatures for CIGS thin film photosensors with 1-μm-thick i-ZnO layers.

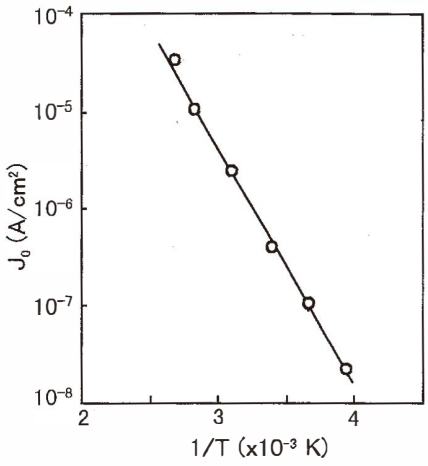

Fig. 5. Temperature dependence of reverse saturation current density for a CIGS thin film photosensor.

$$J_0 = A \exp(-qV_D / kT) \tag{1}$$

Here, V_D: diffusion potential, q: electron charge, k: Boltzmann's constant, $A = (qD_eN_D/L_e) + (qD_hN_A/L_h)$, D_e: electron diffusion coefficient, D_h: hole diffusion coefficient, N_D: hole density, N_A: electron density, L_e: diffusion length of electron, and L_h: diffusion length of hole.

For a CIS crystal, the temperature coefficient of band-gap energy is small, 1.1×10^{-4} eV/K, such that the change of V_D in the temperature range in Fig. 5 is negligible. The temperature dependence of carrier concentration, diffusion length and diffusion coefficient are also assumed to be small. Therefore, A is considered to be almost constant in this temperature range. The temperature coefficient of J_0 is derived from Fig. 5 to be 6.7×10^{-8} (A/cm^2)/K.

On the other hand, the forward current density J observed in Fig. 4 showed straight line dependence for bias voltages in the range of 0.1–0.4 V. The slope of these straight lines is independent of ambient temperature. Similar J-V characteristics have been reported in other heterojunctions such as SnO_2/Si[11] and ITO/Se.[12] In general, this behavior is interpreted as a tunneling process through interface states in the junction area, which is given by the following equation.[10]

$$J = J_0 \exp(\alpha V) \tag{2}$$

Here, $\alpha = \partial lnJ/\partial V$ is a constant which is independent of temperature.

3.3 *Photocurrent vs illumination*

The dependence of the photocurrent on the illumination intensity was measured at room temperature using an A-type standard light source with 2856 K of color temperature (JIS Z8720). The illumination intensity was varied by changing the distance between the photosensors and the light source positioned on an optical bench. Figure 6 showed the short circuit current of the CIGS photosensor under 0 bias voltage as a function of illumination. The linearity in light-current characteristics was obtained for a CIGS sensor under illumination from 1 to 10^3 lux.

3.4 *Photoresponse time*

The photoresponse time was measured using a laser diode pulsed at 20 kHz with a wavelength of 780 nm and an incident power of 1.2 mW. Figure 7 shows a photoresponse curve under zero bias for a CIGS photosensor with 1.0-μm-thick i-ZnO layer. When the bias voltage was 0 V, rise (T_r) and decay times (T_d) were 3.24 and 2.74 μs, respectively. However, when bias voltage was 0.5 V, T_r and T_d became 3.14 and 3.16 μs, respectively. It was also noted that the response time of the CIGS photosensor fabricated in this work was approximately 3 μs which is comparable to the published data of single crystalline silicon (Si) pn junction and amorphous silicon (a-Si) pin junction photodiodes. The chalcopyrite CIGS is a direct transition material so that the response time is essentially higher than indirect transition materials such as Si. However, it is limited by the product of capacitance and series resistance of the diode, including a load resistance (50 Ω in this experiment). The response time and reverse saturation current show a trade-off relation since both of them depend on resistance of the ZnO layer. The capacitance of the CIGS photosensor was 3 nF at 10 kHz under reverse bias voltages ranging from 0.01 to 1.0 V. This result implies that the response time cannot be improved by increasing the reverse bias voltage.

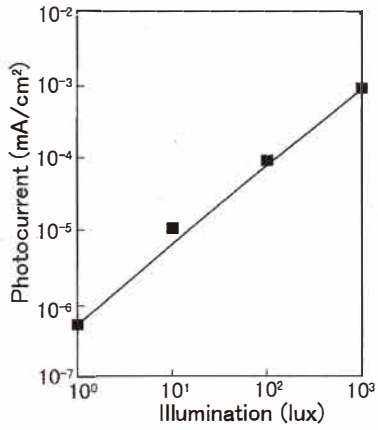

Fig. 6. The photocurrent of a CIGS thin film photosensor as a function of illumination intensity.

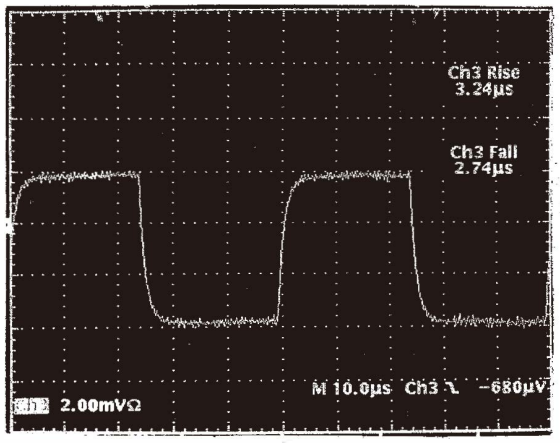

Fig. 7. The photoresponse curve under zero bias for a CIGS thin film photosensor with 1-μm-thick i-ZnO layer.

4. Summary

We have fabricated, for the first time, CIGS thin film photosensors with a ZnO:Al/i-ZnO/CdS/CIGS/Mo/soda-lime glass structure, and have investigated the fundamental sensor characteristics. The comparison in sensor characteristics between CIGS and Si-based photosensors is summarized in Table 1. As can be seen, the photoresponse time of the CIGS sensor is comparable to the Si pn junction or a-Si pin junction photodiodes. It is also evident that the CIGS photosensor has an advantage over Si-based photosensors because of its wider spectral response range. However, the usage of CIGS photosensors will be limited since the dark reverse saturation current is relatively large at present, which results in a small signal-to-noise ratio. We believe that the large dark current can be lowered by increasing the resistivity of the i-ZnO layer and junction properties. According to recently published data, CIGS materials exhibit superior radiation hardness, therefore our CIGS photosensors have a potential for use in space applications.

Table 1
Comparison of sensor characteristics between CIGS and Si-based photosensors.

Junction Structure	Photoresponse wavelengths (nm)	Response Time (μs)	Area (mm^2)	Junction capacitance (PF, 10 KHz)	Reverse saturation current J_0 (A/cm^2)	Ref.
a-Si pin	350–750	1	6	1000	$\sim 10^{-11}$	(13)
Si pn	400–1100	2–8	10	1000	$\sim 10^{-11}$	(14)
CIGS pn	350–1250	3	20	3000	$\sim 10^{-7}$	This work

Acknowledgments

The authors would like to thank Showa Shell Sekiyu K. K. Central R&D Lab. for supplying CIGS/Mo/glass substrates, and Drs. T. Sato and K. Ida of Moririca Electric Ltd. for measurements of photoresponse time. The authors would also like to thank H. Maetsubo and M. Tohno for their assistance with experiments.

References

1 S. Wagner, J. L. Shay and P. Migliorato: Appl. Phys. Lett. **25** (1974) 434.
2 J. R. Tuttle, M. A. Contreras, J. S. Ward, A. M. Gabor, K. R. Ramanathan, A. L. Tennant, L. Wang, J. Keane and R. Noufi: Proc. 1st World Conf. Photovoltaic Energy Conversion (1994) p. 1942.
3 J. Hedstrom, H. Ohlsen, M. Bodegard, A. Kylner and L. Stolt: Proc. 23th Photovoltaic Specialists Conf. (1993) p. 364.
4 T. Hisamatsu, T. Aburaya and S. Matsuda: to be published in Proc. 2nd World Conf. Photovoltaic Energy Conversion (1997).
5 K. Kushiya, S. Kuriyagawa, T. Kase, M. Tachiyuki, I. Sugiyama, Y. Satoh, M. Satoh and H. Takeshita: Proc. 25th IEEE Photovoltaic Solar Energy Conversion (1996) p. 989.
6 Y. Okano, T. Nakada and A. Kunioka: Solar Energy Materials and Solar Cells (1998) 105.
7 D. Schmid, M. Ruckh, F. Grunwald, and H. W. Shock: J. Appl. Phys. **73** (1993) 2902.
8 K. R. Ramanathan, H. Wiesner, D. Niles, R. N. Bhattacharya, J. Keane, M. A. Contreras and R. Noufi: to be published in Proc. 2nd World Conf. Photovoltaic Energy Conversion (1997).
9 T. Nakada, N. Murakami and A. Kunioka: Proc. Materials Research Society Spring Meeting (1996) 411.
10 S. M. Sze: Physics of Semiconductor Devices (John Wiley & Sons, New York, 1969) p. 87.
11 T. Nagatomo, Y. Inagaki, Y. Amano and O. Omoto: Jpn. J. Appl. Phys. **21** (1982) 121.
12 T. Nakada and A. Kunioka: Denshi Tsushin Gakkaishi **J67-C** (1984) 699 [in Japanese].
13 S. Nakano, T. Fukatsu, M. Takeuchi and Y. Kuwano: Proc. 2nd Sensor Symposium (1982) 11.
14 Moririca Electric Limited, Catalogue No. 884G03.